Theoretical Study of the Electronic Structure and Stability of Titanium Dioxide Clusters $(TiO_2)_n$ with $n = 1-9$

Zheng-wang Qu*,† and Geert-Jan Kroes†

Leiden Institute of Chemistry, Gorlaeus Laboratory, Leiden University P.O. Box 9502, 2300 RA Leiden, The Netherlands

Received: November 15, 2005; In Final Form: February 13, 2006

The electronic structure and the stability of both neutral and singly charged $(TiO_2)_n$ clusters with $n = 1-9$ have been investigated using the density functional B3LYP/LANL2DZ method. The lowest-lying singlet clusters tend to form some compact structures with one or two terminal Ti−O bonds, which are about 1.4−2.5 eV more stable than the corresponding triplet structures. For the lowest-lying structures, strong infrared absorption lines at 988−1020 cm^{-1} due to terminal Ti−O bonds and below 930 cm^{-1} due to Ti−O−Ti bridging bonds may be observed, with some characteristic lines at 530−760 cm^{-1} due to 3-fold coordinated O-atoms that are comparable with the spectra of rutile and anatase bulk. The holes and excited electrons within triplet structures tend to be localized on the least coordinated O- and Ti-atoms, respectively, with some exceptions possibly due to the electron−hole interaction. The extra electrons within $(TiO_2)_n^-$ clusters and the holes within $(TiO_2)_n^+$ clusters show a clearer preference of location on the least coordinated Ti- and O-atoms, respectively. For the lowest-lying $(TiO_2)_n$ clusters, the cluster formation energy per TiO_2 unit and the electron affinity tend to increase whereas the ionization potential tends to decrease with the cluster size n. On the other hand, the singlet−triplet and HOMO−LUMO gaps represent the lower and upper limits of the TiO_2 bulk band gaps, respectively. The theoretical results agree well with the available experimental data and may be helpful for understanding the chemistry of small $(TiO_2)_n$ clusters.

1. Introduction

The photooxidation of water at the surface of semiconductor metal oxide photocatalysts such as titanium dioxide TiO_2 nanocrystals may, as a part of photoelectrolysis of water, provide hydrogen as a clean and sustainable energy carrier from solar energy.[1] This process has therefore attracted much attention since the discovery following the early work of Fujishima and Honda.[2] The TiO_2 semiconductor catalyst has a large band gap (3−3.2 eV) and is very stable under illumination for water photolysis, but it absorbs only the ultraviolet part of the solar emission. This can perhaps be remedied by incorporating the photoelectrolysis cell in a tandem cell,[1] and by nitrogen,[3,4] sulfur,[5,6] or carbon[7,8] doping of TiO_2 to extend the photoactivity of the photoanode to the visible region. Furthermore, photochemistry at the surface of TiO_2 also finds application in the removal of organic pollutants.[9] Advantages of TiO_2 are that is inexpensive and chemically and biologically inert.[10]

Normally, TiO_2 may exist in nature as the rutile, anatase and brookite crystals, with rutile being the thermodynamically most stable under ambient conditions.[11] However, if the particle diameters of TiO_2 are smaller than about 14 nm the anatase phase becomes more stable than the rutile phase.[12] If the particles become really small, they may of course have structures that cannot be derived from the bulk. These structures are of interest for several reasons. One reason is that given the cosmic abundances of the elements Ti and O, small $(TiO_2)_n$ clusters are also of astrophysical interest, due to their possible role in dust formation processes in circum-stellar shells of oxygen-rich stars.[13] Another reason for identifying the stable structures of small TiO_2 particles is that they might exhibit interesting quantum size effects on photophysics and substrate−particle interactions. Finally, it is of interest to examine if the stable structures of small TiO_2 particles can be employed in studying photooxidation of water on TiO_2 surfaces, or, more generally, photochemistry on TiO_2 surfaces.

To improve the efficiency and stability of photocatalysts for water oxidation, it is quite important to clarify the detailed mechanism of the photooxidation of water on metal oxide surfaces. Recent experimental data have suggested that the photoevolution of oxygen should be initiated by the nucleophilic attack of a H_2O molecule on a surface-trapped hole.[14,15] From the theoretical point of view, it is thus essential to answer two questions: (1) What are the surface structures in which the photogenerated electrons and holes are trapped, and are these structures found on stable $(TiO_2)_n$ or $(TiO_2)_n^+$ clusters with small n? (2) What are the further molecular processes between water molecules and surface-trapped electrons and holes? Up to now, most theoretical efforts have concentrated on the surface structures of pure or water-adsorbed TiO_2 crystals.[16,17] An additional goal of the present work has been to determine to what extent studies of neutral and charged $(TiO_2)_n$ clusters yield answers to the first question above.

Experimentally, some neutral,[18,19] positively[20,21] and negatively[22] charged titanium oxide clusters have been produced in the gas phase. On the basis of some $(TiO_2)_n$ cluster structures with $n = 1-4$ proposed using a simple pair-potential model,[20] a few ab initio and DFT studies have been performed for small neutral and/or charged $(TiO_2)_n$ clusters with $n = 1-3$.[23−29] Some quasi-linear structures of the neutral $(TiO_2)_n$ clusters with $n = 1-6$ have been calculated using the DFT-B3LYP method,[29] whereas larger $(TiO_2)_n$ nanocrystals in the anatase form with n

† E-mail addresses: z.qu@chem.leidenuniv.nl (Z.-w.Q.) and g.j.kroes@chem.leidenuniv.nl (G.-J.K.).

10.1021/jp056607p CCC: $33.50
Published on Web 04/18/2006

TABLE 1: Predicted Properties for the Ground State TiO and TiO_2 Molecules, Including the Bond Lengths (d_{Ti-O}), Bond Angles (θ), Vibrational Frequencies (ν), Dissociation Energies (D_0), Adiabatic Ionization Potential (IP_a), Adiabatic Electron Affinity (EA_a), and Singlet−Triplet Gaps (Δ_{ST}) (NA = Data Not Available)

	$TiO(^3\Delta)$		$TiO_2(^1A_1)$	
properties	expt	this work	expt	this work
d_{Ti-O} (Å)	1.620[a]	1.634	NA	1.658 (1.672)[h]
θ (deg)			110 ± 5[d]	110.8 (112.6)[h]
ν (cm^{-1})	1009[a]	1046	965, NA, 944[e]	1026, 341, 1007
D_0 (eV)	6.92 ± 0.10[a]	6.86	6.3 ± 0.2[f] 6.1 ± 0.2[j]	5.57
IP_a (eV)	6.819 ± 0.006[b]	7.10	9.5 ± 0.1[g]	9.75
EA_a (eV)	1.30 ± 0.03[c]	1.19	1.59 ± 0.03[c]	1.69
Δ_{ST} (eV)	0.42 ± 0.06[c]	0.25	1.96 ± 0.10[c]	1.94, 1.81[i]

[a] The $TiO(^3\Delta) \rightarrow Ti(^3F) + O(^3P)$ dissociation energy. See ref 40. [b] See ref 41. [c] The value for the TiO^- ($^2\Delta$), TiO ($^1\Delta$), TiO_2^- ($^2A_1$) and TiO_2 ($^3A_2$) species. See ref 22. [d] See ref 42. [e] Symmetric stretch, bending and anti-symmetric stretch modes. See ref 43. [f] The $TiO_2(^1A_1) \rightarrow TiO(^3\Delta) + O(^3P)$ dissociation energy. See ref 44. [g] See ref 44. [h] The CCSD/LANL2DZ values in parentheses. [i] Related to the TiO_2 ($^3A_2$) and TiO_2 ($^3A'$) molecules, respectively. [j] See refs 45 and 46.

taking some values between 16 and 38 have also been proposed, on the basis of general bonding principles applied in a systematic way and B3LYP calculations using larger basis sets.[30] Very recently, the prediction of the global minima of small $(TiO_2)_n$ clusters with $n = 1-15$ has been attempted using a pair-potential model, followed by further DFT-B3LYP geometry optimization of the most stable structures found.[31]

In this work, the electronic structure and stability of both neutral and singly charged $(TiO_2)_n$ clusters with $n = 1-9$ are investigated using the DFT-B3LYP method, and compared with the available experimental and theoretical data. It is shown that both neutral and charged $(TiO_2)_n$ clusters tend to form stable compact rather than quasi-linear structures[29] for increasing cluster sizes n, with one or two terminal Ti−O bonds. Moreover, the excited electron within triplet clusters and the extra electron within negatively charged clusters tend to be localized on the least-coordinated Ti-atom(s), whereas the holes within triplet clusters and positively charged clusters tend to be localized on the terminal O-atom(s).

2. Computational Methods

All calculations are done using the GAUSSIAN 03 program.[32] First, the geometries of both singlet and triplet neutral $(TiO_2)_n$ clusters are fully optimized at the hybrid density functional theory (DFT) level.[33] The Becke's three-parameter exchange functional[34] along with the Lee−Yang−Parr's correlation functional,[35] i.e., B3LYP functional, and the standard LANL2DZ basis set[36−39] is chosen in all our calculations. The accuracy of our method has been tested by comparison to experiment and ab initio calculations for TiO and TiO_2. The LANL2DZ basis set involves the D95 basis set on oxygen[36] and the Los Alamos effective core potential plus double-ζ basis set[37−39] on titanium, respectively, leading to 40 basis functions with 103 primitive Gaussians per TiO_2 unit in our calculations. Subsequent harmonic vibrational frequency analysis is used to identify the nature of optimized stationary points as real local minima (without any imaginary frequency), transition states (with only one imaginary frequency) or higher-order saddle points (with more than one imaginary frequency).

Single-point B3LYP calculations are performed for (both negatively and positively) singly charged clusters using the optimized geometries of neutral $(TiO_2)_n$ clusters to evaluate the vertical electron affinities (EA_v) and ionization potentials (IP_v). Subsequently, full optimization and frequency analysis are performed for the charged clusters to give the adiabatic electron affinities (EA_a) or ionization potentials (IP_a) of stable neutral clusters. Mulliken's population analysis is performed using the SCF density of the optimized clusters. The locations of holes and excited electrons within the triplet clusters are inferred from the calculated atomic spin densities and from the analysis of the singly occupied frontier molecular orbitals. Similar analysis is also performed for the location of the extra electrons within the $(TiO_2)_n^-$ clusters and the holes within the $(TiO_2)_n^+$ clusters. Note that in the following discussions, all energies are corrected by the zero-point energies (ZPE) derived from our frequency analysis, except for the EA_v and IP_v values.

3. Results and Discussions

For clarity, in the bonding analysis below we assume that one Ti−O bond exists if the Ti−O distance is smaller than 2.15 Å, and that one Ti−Ti bond exists if the Ti−Ti distance is smaller than 2.90 Å. For comparison, the shortest Ti−O and Ti−Ti distances in rutile are 1.95 and 2.96 Å, respectively.[11] The coordination number of one Ti- or O-atom is defined as the number of its surrounding Ti−O bonds. In section 3.1, the reliability of the B3LYP/LANL2DZ method for predicting properties of $(TiO_2)_n$ clusters is tested using both neutral and singly charged TiO and TiO_2 molecules, which are known to be challenging for quantum chemical methods in general.[23,27] In section 3.2, the low-lying singlet $(TiO_2)_n$ clusters with $n = 2-9$ are discussed, whereas the infrared spectra of the global minima are presented in section 3.3. The results for the triplet neutral clusters, negatively charged clusters and positively charged clusters are described in sections 3.4−3.6, respectively.

3.1. Test Calculations: TiO and TiO_2 Molecules. As shown in Table 1 and Figure 1, the calculated bond length of the triplet ground state of $TiO(^3\Delta)$ is 1.634 Å, in good agreement with experiment.[40] The singlet ground state of the TiO_2 molecule, labeled as **1a** (C_{2v}, $^1A_1$) (Figure 1) with molecular symmetry and electronic state in parentheses, has two equal Ti−O bond lengths of 1.658 Å with a O−Ti−O angle of 110.8 degrees. Experimentally, only an estimate exists of the O−Ti−O angle (110 ± 5°).[42] For the ground state of TiO_2, our B3LYP geometries agree well with the highly correlated CCSD results (Table 1). The cyclic isomer of TiO_2, **1b** (C_{2v}, $^1A_1$), lies 4.73 eV above **1a** in energy. The O−O bond within **1b** may break over a very small barrier of 0.11 eV via a transition state of C_s symmetry, suggesting a very poor kinetic stability. Two triplet minima of the TiO_2 molecule are found to be very close in energy, with ^{3}**1a**′ (C_s, $^3A'$) being only 0.13 eV below ^{3}**1a** (C_{2v}, $^3A_2$) in energy. The TiO_2 (C_{2v},$^3B_2$) structure is found to be unstable, deforming into ^{3}**1a**′. Two different triplet structures have been found in previous B3LYP/DZP calculations,[27] one with $D_{\infty h}$ symmetry and the other with C_{2v} symmetry; however, they are here identified as second- and first-order saddle points,

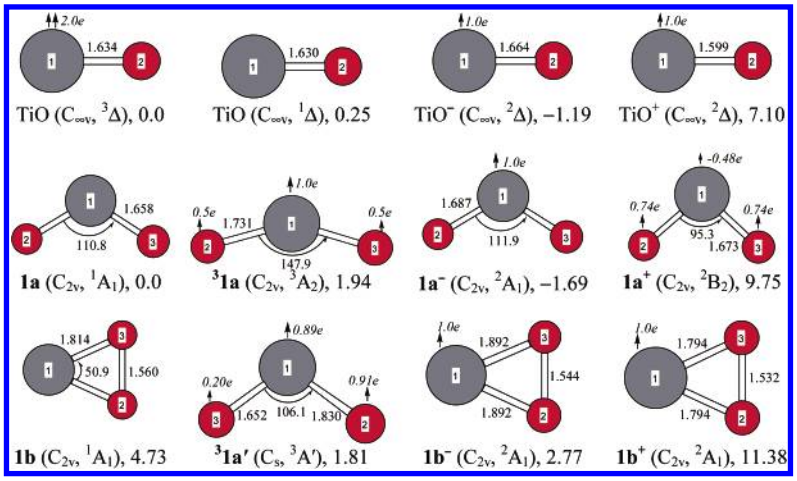

Figure 1. Geometries of neutral and singly charged TiO and TiO_2 molecules. The Ti-atoms are indicated by gray spheres (labeled by 1) and the O-atoms by red spheres. All bond lengths are in Å and angles in degrees. The point groups and electronic states are given in parentheses, whereas the energies (in eV) relative to the corresponding neutral ground states are given after the comma. The main spin densities of open-shell structures are indicated by arrows.

respectively, and may lead to ^{3}**1a** and ^{3}**1a**′ after full geometry optimization in our calculations.

A more detailed comparison of the calculated energetics is given in Table 1. The computed vibrational frequencies are too high by about 6% compared to experiment.[40,43] Overall, the predicted dissociation energies, IP_a and EA_a values, and the singlet−triplet gaps are within about 0.2 eV of the experimental data.[22,40,41,44] Excellent agreement between theory and experiment is observed for the TiO ($^3\Delta$) → Ti (^{3}F) + O (^{3}P) dissociation energy[40] and the singlet−triplet gap of TiO_2.[20] The TiO_2 ($^1A_1$) → TiO ($^3\Delta$) + O (^{3}P) dissociation energy is underestimated by about 0.5 eV in our calculations as compared with the experimental values of 6.1−6.3 eV,[44−46] which is still much improved over previous ab initio (HF, MP2, CISD)[27] and DFT-LDA[23] results with errors larger than 2 eV in these cases. The energies of ^{3}**1a**′ and ^{3}**1a** relative to the ground state of TiO_2^-, **1a**$^-$ (C_{2v}, $^2A_1$), are 3.50 and 3.63 eV, respectively, which may be responsible for the observed peaks around 3.4 and 3.6 eV in the photoelectron spectra.[22] The excellent reliability of the B3LYP/LANL2DZ method for the TiO and TiO_2 molecules suggests its applicability to larger $(TiO_2)_n$ clusters.

3.2. Singlet $(TiO_2)_n$ Clusters with $n = 2-9$. Though some possible structures have been proposed for the $(TiO_2)_n$ clusters with $n = 2-4$ using a pair-potential model,[20] many more initial structures are constructed in this work to identify the true global minima. The lowest-lying structures of the $(TiO_2)_n$ clusters are found always in the singlet ground state, whereas the corresponding triplet structures are at least 1.4 eV higher in energy. A learning-and-application strategy is used to construct the low-lying structures: First, it is not too difficult to imagine the possible structures of small clusters with $n = 2-4$, with the Ti-atoms being at least 2-fold coordinated. Second, the low-lying structures found are used as the building blocks for larger clusters, whereas some energetically unfavorable features such as O−O bonds and more than three terminal Ti−O bonds are avoided. Geometry optimizations were performed for a large range of initial geometries without symmetry constrains. This way, we have identified 4, 8, 13, 14, 13, 15, 8 and 8 low-lying singlet isomers for the $(TiO_2)_n$ clusters with $n = 2-9$, respectively.

Figure 2 shows the three lowest-lying isomers for each $(TiO_2)_n$ clusters. A common feature is that these lowest-lying clusters always possess one or two terminal Ti−O bonds of almost constant length (∼1.63 Å). On the other hand, the bond lengths of other Ti−O and Ti−Ti bonds may vary between 1.70 and 2.10 Å and between 2.45 and 2.90 Å, respectively, dependent on the particular chemical environments. The details are given below.

For the $(TiO_2)_2$ cluster, the structure **2a** (C_{2h}, ^1A_g) with two terminal Ti−O bonds is identified as the global minimum, in agreement with previous DFT-LDA[23] and B3LYP[29] calculations. The Ti−O bond lengths in the TiO_2Ti rhombus are 1.85 Å, about 0.2 Å longer than those of terminal Ti−O bonds. Its cis-counterpart, **2b** (C_{2v}, $^1A_1$) is 0.28 eV above **2a** in energy, with a small barrier of 0.28 eV toward **2a** via inversion of one $OTiO_2$ pyramid. The structure **2c** (C_{3v}, $^1A_1$) with one terminal and three bridging O-atoms has also been found in previous DFT-LDA calculations.[23] It is 0.85 eV above **2a** in energy, with almost no barrier (smaller than 0.01 eV) toward **2a**. Other structures, with O−O bonds and/or with more than three bridging O-atoms,[20] are found to be at least 4 eV above **2a** in energy; in addition, the cleavage of an O−O bond may occur typically over a very small barrier of about 0.1 eV.

For the $(TiO_2)_3$ cluster, the structure **3a** (C_s, $^1A'$) with two terminal and one 3-fold coordinated O-atom is identified as the global minimum, in agreement with previous DFT-LDA calculations.[23] The structure **3b** (C_1, ^1A), with topology similar to that of **3a** but without a 3-fold coordinated O-atom, is 0.13 eV above **3a** in energy with a very small barrier of 0.06 eV toward **3a** via an additional Ti−O bond. The third structure **3c** (C_2, ^1A) resembles the quasi-linear isomer with two orthogonal TiO_2-Ti rhombi in previous B3LYP calculations.[29] It is 0.37 eV above **3a** in energy and may convert into isomer **3b** over a sizable barrier of 0.79 eV via bending its quasi-linear skeleton. Note that **3c** was suggested to represent the global minimum in early Hartree−Fock (HF)[26] and pair-potential[20] studies, whereas **3b** was suggested as global minimum in a recent pair-potential study.[31] Given the much better performance of the B3LYP over the HF method for titanium oxide clusters,[27] the pair-potential models[20,31] seem unreliable for predicting the lowest-lying structures, due to the neglect of the partial covalent nature of Ti−O bonds. This is indeed observed for larger $(TiO_2)_n$ clusters, as will be discussed below.

The structure **4a** (C_{2v}, $^1A_1$) with two terminal and six bridging O-atoms is identified as the global minimum of the $(TiO_2)_4$ cluster. Another C_{2v} isomer **4b** already shows some ionic character with one 4-fold coordinated O-atom, because normally the coordination number of oxygen does not exceed three in

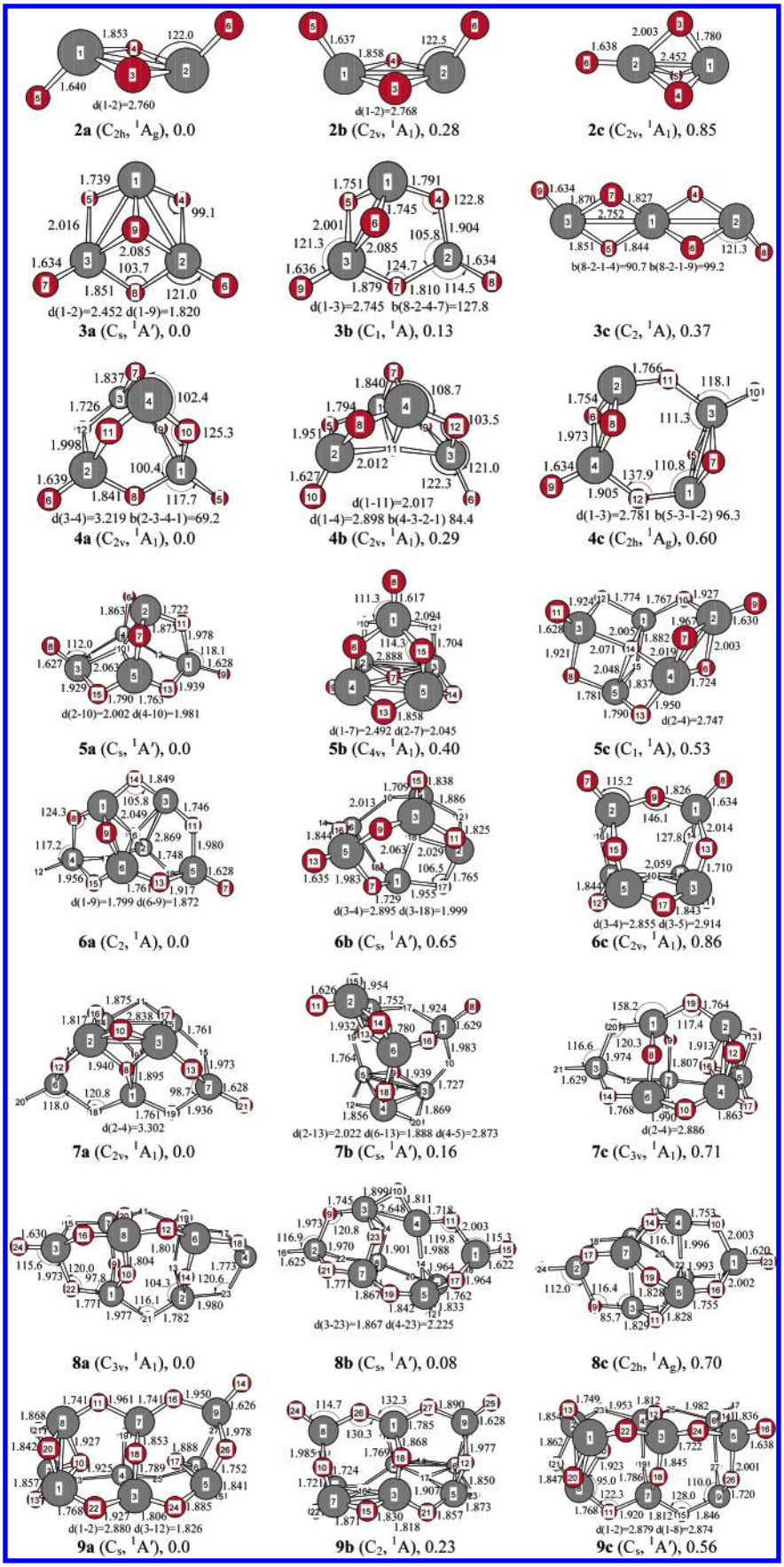

Figure 2. Geometries of three lowest-lying isomers of each neutral singlet $(TiO_2)_n$ cluster with $n = 2-9$. The Ti-atoms are indicated by gray spheres and labeled by the numbers from 1 to n; the O-atoms are indicated by red spheres. Some bond lengths are indicated in parentheses preceded by "d". Other details are the same as in Figure 1.

covalent compounds. In fact, it is 0.29 eV above **4a** in energy though it has recently been suggested as the global minimum.[31] The third stable structure, **4c** (C_{2h}, ^1A_g) may represent a general way to construct low-lying $(TiO_2)_n$ clusters by just piling up $n/2$ $(TiO_2)_2$ units (i.e., the C_{2h} structure **2a**). Note that **4c** is 0.60 eV above **4a** in energy but still 0.7 eV below a suggested quasi-linear $(TiO_2)_4$ structure.[29] Other proposed low-lying structures[20] either are high-order saddle points or are too high-lying in energy according to our calculations.

As can be seen from Figure 2, all three lowest-lying isomers of $(TiO_2)_5$ exhibit ionic character in that they possess a 4-fold coordinated O-atom. The isomer **5a** (C_s, $^1A'$) with two terminal and seven bridging O-atoms is the global minimum, in agreement with the pair-potential results.[31] The highly symmetric structure **5b** (C_{4v}, $^1A_1$) shows very interesting bonding character, with one 4-fold coordinated O-atom in almost the same plane with four Ti-atoms and four bridging O-atoms and with a shortest (1.617 Å) terminal Ti−O bond connected to a 5-fold coordinated Ti-atom. Similarly to **5a**, all Ti-atoms within the third structure **5c** (C_1, ^1A) are 4-fold coordinated. For comparison, the isomer **5c** is 0.53 and 0.13 eV above **5a** and **5b** in energy, respectively, but it is still 1.28 eV below the suggested quasi-linear structure with C_2 symmetry.[29]

For the $(TiO_2)_6$ cluster, the lowest-lying isomers **6a** (C_2, ^1A), **6b** (C_s, $^1A'$), and **6c** (C_{2v}, $^1A_1$) show some common bonding features: all Ti-atoms are 4-fold coordinated, and there is one 4-fold coordinated O-atom and two terminal Ti−O bonds. The identified global minimum **6a** is 0.65 and 0.86 eV more stable than **6b** and **6c**, respectively, and it is 1.66 eV below the recently suggested[31] global minimum. For comparison, another high-lying structure constructed by piling up three $(TiO_2)_2$ units, similar to the way structure **4c** (C_{2h}, ^1A_g) can be obtained from **2a**, is 1.76 eV above **6a** but still 1.67 eV below the suggested[29] quasi-linear structure of $(TiO_2)_6$ (C_{2h}, ^1A_g) in energy.

From the discussion above, it is clearly seen that some compact rather than quasi-linear structures become energetically more and more favorable for increasing cluster sizes n. Therefore, only compact isomers are constructed and tested for the $(TiO_2)_n$ clusters with $n = 7-9$, with the Ti-atoms to be no less than 3-fold coordinated and the O-atoms to be no more than 4-fold coordinated.

For the $(TiO_2)_7$ cluster, both the structures **7a** (C_{2v}, $^1A_1$) and **7b** (C_s, $^1A'$) possess two terminal and two 3-fold coordinated O-atoms as well as seven 4-fold coordinated Ti-atoms, with the former being only 0.16 eV more stable. The third structure **7c** (C_{3v}, $^1A_1$) with only one terminal O-atom is 0.71 eV above **7a** but still 0.71 eV below the suggested[31] global minimum with C_2 symmetry in energy! The efforts to find $(TiO_2)_7$ isomers without terminal O-atoms and/or with more than 5-fold coordinated Ti-atoms always lead to higher-lying $(TiO_2)_7$ isomers.

For the $(TiO_2)_8$ cluster, the two lowest-lying structures **8a** (C_{3v}, $^1A_1$) and **8b** (C_s, $^1A'$) have very similar arrangements of the Ti-atoms but a different number of terminal Ti−O bonds. The isomer **8a** has only one terminal Ti−O bond but no highly coordinated O-atoms whereas **8b** has two terminal and one (or three, if Ti−O bonds longer than 2.23 Å are counted) 3-fold coordinated O-atom. They are very close in energy, with the former being only 0.08 eV more stable. The structure **8c** (C_{2h}, ^1A_g), with two terminal and two 3-fold coordinated O-atoms, is 0.70 eV above **8a** in energy. The structure with two 6-fold coordinated Ti-atoms but no terminal O-atoms, suggested as global minimum in ref 31, is only 0.13 eV less stable than **8a** according to our calculations. This fact suggests that low-lying structures with highly coordinated Ti-atoms and/or without terminal O-atoms are also possible for larger $(TiO_2)_n$ clusters. The structure with two 6-fold coordinated Ti-atoms[31] was at first not found in our own calculations.

TABLE 2: Cluster Formation Energies per TiO_2 Unit (E_c), Singlet−Triplet Gaps (Δ_{ST}), HOMO−LUMO Gaps (E_{HL}), Vertical and Adiabatic Electronic Affinities (EA_v and EA_a), Vertical and Adiabatic Ionization Potentials (IP_v and IP_a) for the Global Minima of $(TiO_2)_n$ with $n = 2-9$ (All Energy Data in eV)

n	E_c	Δ_{ST}	Δ_{ST}-(expt)[b]	E_{HL}	EA_v	EA_a	EA_a(expt)[c]	IP_v	IP_a
2	2.41[a]	2.14	2.0	4.89	1.74	2.12	2.10 ± 0.08	10.44	9.91[d]
3	3.23	1.70	1.8	3.69	2.86	3.32	2.9 ± 0.1	10.13	9.69
4	3.79	1.44	1.6	3.15	2.89	3.44	3.3 ± 0.2	9.35	8.88
5	4.05	2.17		4.54	2.56	3.24		10.44	9.54
6	4.41	1.96		4.53	2.92	3.68		10.49	9.55
7	4.48	1.65		3.96	3.35	3.92		10.19	9.30
8	4.48	1.59		3.58	3.04	3.90		9.50	8.27
9	4.71	2.50		3.84	3.11	3.94		9.94	8.69

[a] The experimental value is 2.58 ± 0.34 eV, as derived from refs 45 and 46. [b] The values approximately read from Figure 8 of ref 22, from which the small peaks slightly before the second arrows are assigned to the lowest triplet states. [c] See Table 3 of ref 22. [d] The experimental value is 10.0 ± 0.5 eV. See ref 46.

For the $(TiO_2)_9$ clusters, the three lowest-lying structures of **9a** (C_s, $^1A'$), **9b** (C_2, ^1A) and **9c** (C_s, $^1A'$), are all compact structures with only 4-fold coordinated Ti-atoms and with one or two terminal Ti−O bonds. These $(TiO_2)_9$ isomers are very close in energy, with the global minimum **9a** being only 0.23 and 0.56 eV more stable than **9b** and **9c**, respectively. The recently suggested global minimum,[31] with highly coordinated Ti-atoms and one terminal Ti−O bond, is also found in our calculations, but at 1.01 eV above **9a** in energy.

Within the normal rutile and anatase forms of TiO_2 crystal, the Ti- and O-atoms are six- and 3-fold coordinated, respectively. Higher coordination numbers of titanium and oxygen atoms can be found only in some high-pressure phases such as fluorite.[11] The structures **3a**, **7a**, and **9a** in this work resemble rutile and anatase in that they possess 3-fold coordinated O-atoms whereas the structures **5a** and **6a** resemble fluorite in that they exhibit 4-fold coordinated O-atoms. However, the 6-fold or 5-fold coordinated Ti-atoms (the later with all O-atoms below them) found within TiO_2 bulk or stable surfaces, are not found in our lowest energy clusters with up to nine TiO_2 units.

As shown in Table 2, the calculated cluster formation energy, per TiO_2 unit, of the lowest-lying $(TiO_2)_n$ clusters with $n = 2-9$ increases monotonically with the cluster size n. The smallest value of 2.41 eV is predicted for the $(TiO_2)_2$ cluster, which agrees well with the experimental value of 2.6 ± 0.3.[45,46] On the other hand, the largest value of 4.71 eV computed for the $(TiO_2)_9$ cluster, is still about 1.91 eV smaller than that of TiO_2 bulk.[47,48]

3.3. Infrared Spectra of the Most Stable $(TiO_2)_n$ Clusters. On the basis of the test calculations for the TiO ($^3\Delta$) and TiO_2 ($^1A_1$) molecules, the theoretical frequencies have been scaled by a factor of 0.95 for better comparison with the experimental spectra of rutile and anatase.[48] Note that only the relative intensities of allowed electric dipole transitions are shown in the predicted infrared spectra as shown in Figure 3. It can be seen that the $(TiO_2)_n$ minimum energy clusters with $n = 2-9$ may show some strong infrared absorption lines between 990 and 1030 cm^{-1} due to the stretching of terminal Ti−O bonds, and between 500 and 900 cm^{-1} mainly due to the stretching of Ti−O−Ti bonds. For example, the strong absorption lines at 645 (a_u) and 706 (b_u) cm^{-1} observed in the spectra of the $(TiO_2)_2$ (**2a**) cluster are due to the vibrations of the TiO_2Ti rhombus

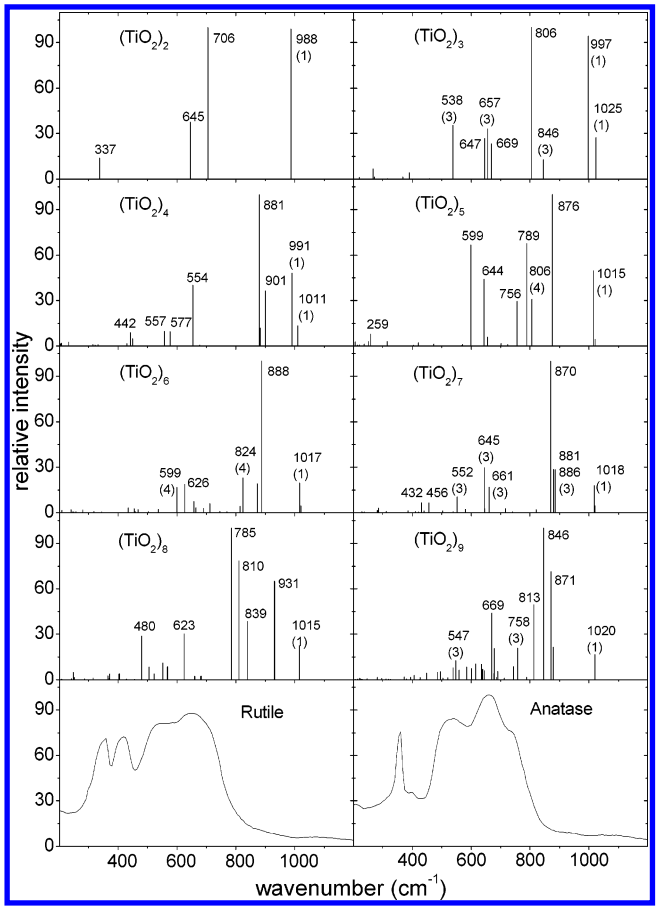

Figure 3. Infrared spectra of the most stable $(TiO_2)_n$ clusters with $n = 2-9$. Note that the calculated frequencies have been scaled by a factor of 0.95 for better comparison. For clarity, the absorption peaks due to the vibrations involving 1-, 3- and 4-fold coordinated O-atoms are indicated by (1), (3) and (4), respectively.

and the 988 (b_u) cm^{-1} line is due to the anti-symmetric combination of the vibrations of two terminal Ti−O bonds; the weak line at 337 cm^{-1} is due to the deformation of the whole molecular skeleton. For larger clusters without highly coordinated O-atoms, such as the $(TiO_2)_4$ (**4a**) and $(TiO_2)_8$ (**8a**) clusters, the strong absorption lines of Ti−O−Ti bonds may be blue-shifted by about 100−330 cm^{-1}.

The $(TiO_2)_5$ (**5a**) and $(TiO_2)_6$ (**6a**) clusters containing 4-fold coordinated O-atoms show some characteristic lines at 806 cm^{-1} and at 599 and 824 cm^{-1}, respectively, though these peaks are still 2−6 times weaker than the strongest lines due to Ti−O−Ti bonds at 876 cm^{-1} (**5a**) and at 888 cm^{-1} (**6a**). On the other hand, the $(TiO_2)_3$ (**3a**) cluster shows some characteristic lines at 538, 657 and 846 cm^{-1} due to vibrations involving a three-coordinated O-atom and at 647, 669 and 806 cm^{-1} due to vibrations of Ti−O−Ti bonds. Similar characteristic lines involving the vibrations of three-coordinated O-atom(s) are also observed for the $(TiO_2)_7$ (**7a**) cluster at 552, 645, 661, 881 and 886 cm^{-1} and for the $(TiO_2)_9$ (**9a**) cluster at 547 and 758 cm^{-1}, respectively, which are comparable with the broad infrared peaks of the bulk of the rutile phase at 539 and 652 cm^{-1} and of the anatase phase at 540, 660 and 740 cm^{-1}.[48]

3.4. Triplet $(TiO_2)_n$ Clusters with $n = 2-9$. Figure 4 shows the fully optimized geometries of triplet $(TiO_2)_n$ clusters corresponding to the singlet global minima with $n = 2-9$. These triplet structures except for ^{3}**9a** (C_1, ^{3}A) may be regarded as the result of exciting one electron from one terminal O-atom to one Ti-atom not too far away within the corresponding singlet structures, leading to lower molecular symmetry. The structure

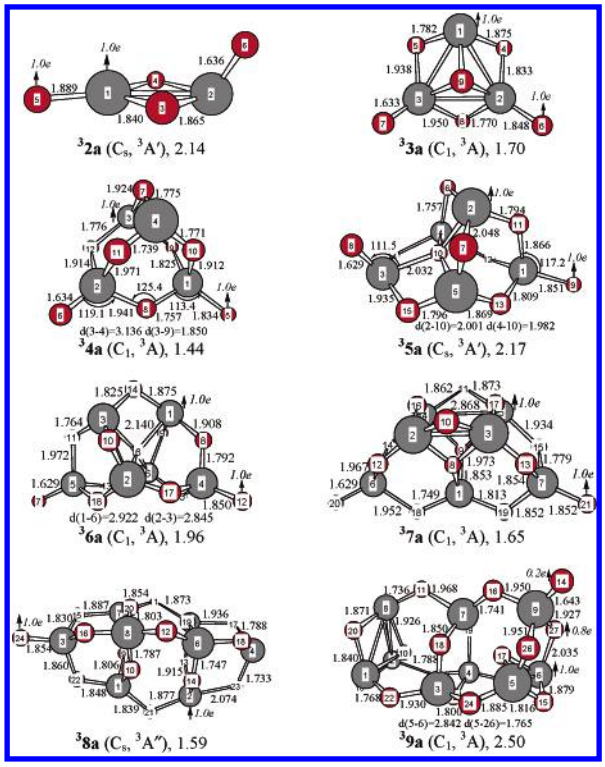

Figure 4. Geometries of the triplet $(TiO_2)_n$ clusters corresponding to the lowest-lying singlet counterparts with $n = 1-9$, as well as the singlet−triplet gaps in eV. Other details are the same as in Figures 1 and 2.

^{3}**2a** (C_s, ^{3}A′) shows the shortest separation between the excited electron and hole, of only one Ti−O bond that is elongated by 0.25Å as compared with it singlet counterpart **2a**. For each of the triplet $(TiO_2)_n$ clusters with $n = 3-7$, the excited electron and hole are separated by three Ti−O bonds, with the terminal Ti−O bond being elongated by about 0.22 Å. The excited electron and hole within the triplet structure ^{3}**8a** (C_s, ^{3}A") are separated by five Ti−O bonds, the largest electron−hole separation found among all triplet structures. Different from other triplet structures, the excited electron within ^{3}**9a** (C_1, ^{3}A) is from one bridging O-atom, which belongs to a short Ti−O bond (1.752 Å) within the singlet structure **9a** (C_s, ^{1}A′) that is longer by 0.28 Å within ^{3}**9a** (C_1, ^{3}A). Other Ti−O bonds are alternately elongated and shortened, by 0.1−0.2 Å for connecting bonds but by less for bonds not directly connecting the excited electron and hole. The Ti−O bonds being more than three Ti−O bonds away from both the excited electron and hole are almost not influenced.

The singlet−triplet gaps of $(TiO_2)_n$ clusters with $n = 2-4$ have been determined by anion photoelectron spectroscopy to be in the range 1.6−2.0 eV.[22] These measured values were previously related to the HOMO−LUMO gaps of the $(TiO_2)_n$ clusters,[22] leading to the surprising conclusion that the HOMO−LUMO gaps were presumably smaller than the TiO_2 bulk band gaps of about 3.0−3.2 eV.[49] To our knowledge, the singlet−triplet gaps have been calculated only for the $(TiO_2)_2$ and $(TiO_2)_3$ clusters with constrained symmetry for both singlet and triplet structures.[23,24]

As can be seen from Table 2, the singlet−triplet gaps we predict are 2.14, 1.70 and 1.44 eV for the $(TiO_2)_n$ clusters with $n = 2-4$, respectively, which agrees very well with the experimental values of 2.0, 1.8 and 1.6 eV[22] and thus much better than the previously calculated values of 3.48 and 2.52 eV for $n = 2$, 3.[23,24] The more or less similar singlet−triplet

gaps for $n = 2-4$ can be due to the similar location of the excited electron and hole within triplet structures. For larger $(TiO_2)_n$ clusters, the predicted singlet−triplet gaps are 2.17, 1.96, 1.65, 1.59 and 2.50 eV for $n = 5-9$, respectively, whereas no experimental data are available. On the other hand, the predicted HOMO−LUMO gaps fluctuate somewhat irregularly between 3.15 and 4.89 eV for small $(TiO_2)_n$ clusters with $n = 2-9$, though decreasing values may be expected for larger clusters according to the normal quantum size effects.[17] The largest HOMO−LUMO gap (4.89 eV) is observed for the $(TiO_2)_2$ cluster whereas the smallest one (3.15 eV) is observed for the $(TiO_2)_4$ cluster. It seems that the singlet−triplet and HOMO−LUMO gaps may represent lower and upper limits to the TiO_2 bulk band gaps,[49] respectively.

3.5. Negatively Charged $(TiO_2)_n^-$ Clusters. Figure 5 shows the optimized geometries for some lowest-lying negatively charged $(TiO_2)_n^-$ clusters corresponding to the low-lying singlet neutrals, in the sense that the geometry optimization was in each case started from the minimum energy structure of the neutral. A common feature is that the extra electron within each $(TiO_2)_n^-$ cluster tends to be localized on the least coordinated Ti-atom, with only one exception, i.e., **4a**$^-$ (C_{2v}, $^2A_1$) in which the extra electron is delocalized between two 3-fold coordinated Ti-atoms to form an additional Ti−Ti bond. The extra electron in the **8a**$^-$ (C_{3v}, $^2A_1$) cluster is localized on the 3-fold coordinated Ti-atom, instead of on the 4-fold coordinated one as in the triplet structure ^{3}**8a** (C_s, $^3A''$). Different locations of the unpaired electron are also observed for the structures **9a**$^-$ (C_1, ^2A) and ^{3}**9a** (C_1, ^3A), which may be due to the additional interaction between the excited electron and the hole within triplet structures. The Ti−O bonds directly around the location of the extra electron within the $(TiO_2)_n^-$ clusters are elongated whereas other Ti−O bonds away from the location of extra electron are alternately shortened and elongated compared to those within the singlet $(TiO_2)_n$ clusters, to a degree decreasing with increasing distance from the extra electron.

For most $(TiO_2)_n^-$ clusters, the negatively charged structures corresponding to the singlet global minima are still the global minima, with one exception: the negatively charged structure **8a**$^-$ (C_{3v}, $^2A_1$) is 0.59 eV less stable than **8b**$^-$ (C_1, ^2A) whereas the corresponding neutral structures **8a** (C_{3v}, $^1A_1$) and **8b** (C_s, $^1A'$) are very close in energy (within 0.08 eV). For the $(TiO_2)_2^-$ cluster, the geometric relaxation of the negatively charged structure **2b**$^-$ always leads to **2a**$^-$ (C_s, $^2A'$), which is 0.59 eV more stable than **2c**$^-$ (C_{3v}, $^2A_1$). Similarly, for the $(TiO_2)_3^-$ cluster the structure **3b**$^-$ is optimized into **3a**$^-$ (C_s, $^2A'$), which is 1.07 eV more stable than **3c**$^-$ (C_s, $^2A'$).

The calculated EA_v and EA_a data for the lowest-lying $(TiO_2)_n$ clusters with $n = 2-9$ are shown in Table 2. The EA_a values are 2.12, 3.32 and 3.44 eV for the cluster size $n = 2-4$, respectively, which mostly agrees well with the experimental data of 2.10 ± 0.08, 2.9 ± 0.1, and 3.3 ± 0.2 eV.[22] Previous DFT-LDA calculations with constrained symmetry led to too low EA_a values of 1.27 for the $(TiO_2)_2$ cluster and 2.31 eV for the $(TiO_2)_3$ cluster.[23] There are no electron affinity data for larger $(TiO_2)_n$ clusters in the literature. The computed electron affinities, especially the EA_a values, tend to increase monotonically with the cluster size n, indicating the importance of electron redistribution and geometric relaxation.

3.6. Positively Charged $(TiO_2)_n^+$ Clusters. Figure 6 shows the optimized positively charged $(TiO_2)_n^+$ clusters corresponding to the low-lying singlet neutrals, in the sense that the geometry optimization was in each case started from the minimum energy structure of the neutral. A common feature is that the hole within each $(TiO_2)_n^+$ cluster is always localized on one terminal O-atom, leading to an elongated (by about 0.2 Å) terminal Ti−O bond as compared with the singlet neutral counterpart; other Ti−O bonds surrounding this terminal one are alternately shortened and elongated to a degree decreasing with increasing distance from the hole. Note that the hole is localized on one terminal O-atom within the structure **9a**$^+$ (C_s, $^2A'$), but on one bridging O-atom within the triplet structure ^{3}**9a** (C_1, ^3A), probably also due to the additional electron−hole interaction in the triplet structure. Upon ionization, the order of stability is reversed for the **6a**$^+$ (C_1, ^2A) and **6b**$^+$ (C_1, ^2A) and for **9a**$^+$ (C_s, $^2A'$) and **9c**$^+$ (C_1, ^2A), as compared with their singlet neutral counterparts.

The localization of the hole at terminal O-atoms in the lowest-lying $(TiO_2)_n^+$ clusters with $n = 2-9$ presented in Figure 6 rules these clusters out as suitable models for modeling photooxidation of water on TiO_2. In a mechanism recently suggested,[14] the hole resides close to a surface bridging O-atom. Stable TiO_2 surfaces relevant to photooxidation of water do not exhibit terminal Ti−O bonds, but bridging O-atoms, and at any rate terminal Ti−O bonds are unstable in water. In a $(TiO_2)_n^+$ cluster that would be useful for studying photooxidation of water, the hole would therefore be localized near a bridging O-atom, and not on a terminal O-atom.

The calculated IP_v and IP_a data for the global minima of the $(TiO_2)_n$ clusters with $n = 2-9$ are listed in Table 2. The IP_a value of 9.91 eV for the $(TiO_2)_2$ (**2a**) cluster agrees very well with the experimental value of 10.0 ± 0.5 eV.[46] For comparison, previous DFT-LDA calculations with the symmetry of both the $(TiO_2)_2$ and the $(TiO_2)_2^+$ clusters constrained to C_{2h} led to a smaller IP_a value of 9.6 eV.[23] No experimental data are available for the larger $(TiO_2)_n$ clusters. The predicted IP_v and IP_a values tend to decrease monotonically with the cluster size n, with the $(TiO_2)_4$ (**4a**) cluster as an exception to this trend.

In experiments in which titanium foil was sputtered in a high-pressure (0.1−0.2 Torr) fast-atom bombardment ion source with an O_2 pressure larger than 0.25 mbar, the oxygen-deficient $Ti_nO_{2n-1}^+$ rather than stoichiometric $(TiO_2)_n^+$ clusters have been observed as the only abundant species.[20] According to our calculations, this can be partly explained by the low stability of $(TiO_2)_n^+$ clusters with respect to the loss of one O-atom from the elongated terminal Ti−O bond during collisions with bath gases. For example, it needs only 2.91, 3.11 and 3.50 eV to remove one terminal O-atom from TiO_2^+, $(TiO_2)_2^+$ and $(TiO_2)_3^+$, but 5.57, 6.81 and 5.74 eV from their singlet neutral counterparts, respectively. On the other hand, the remaining terminal Ti−O bonds within $Ti_nO_{2n-1}^+$ with $n = 1-3$ are found to be slightly shortened and thus may be stronger than those within $(TiO_2)_n$ clusters.

4. Conclusions

The electronic structure and stability of neutral $(TiO_2)_n$ as well as of singly charged $(TiO_2)_n^-$ and $(TiO_2)_n^+$ clusters with $n = 1-9$ have been investigated using the density functional B3LYP/LANL2DZ method. For all $(TiO_2)_n$ clusters with $n = 1-9$, the global minima are always found in the singlet ground state, with the corresponding triplet structures being about 1.4−2.5 eV less stable. For increasing cluster size n, compact structures with one or two terminal O-atoms become increasingly energetically favored. For the lowest-lying structures, strong infrared absorption lines at 988−1020 cm^{-1} due to terminal Ti−O bonds and below 930 cm^{-1} due to Ti−O−Ti bridging bonds may be observed, with some characteristic lines at 530−760 cm^{-1} due to 3-fold coordinated O-atoms that occur

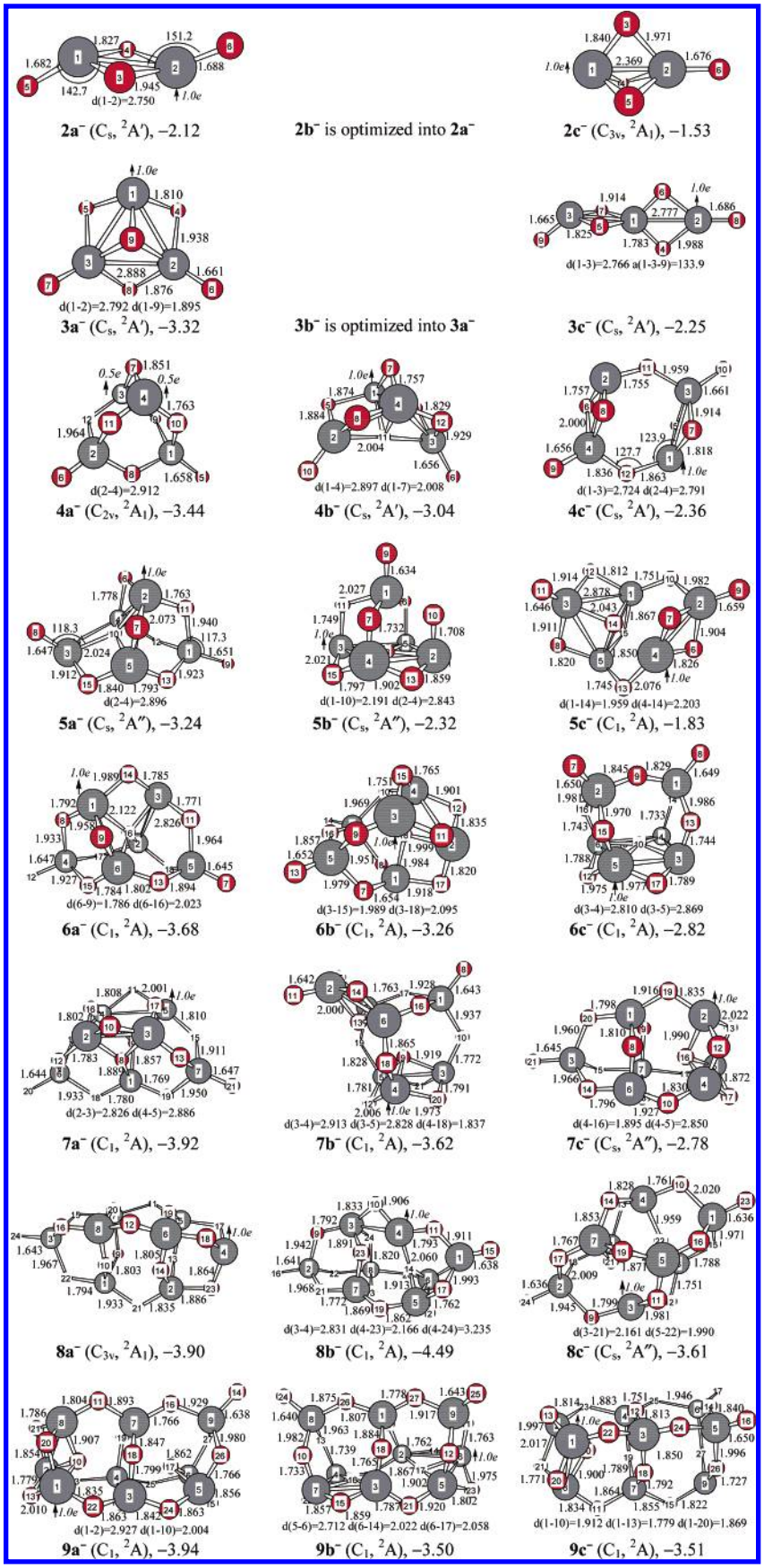

Figure 5. Geometries of negatively charged $(TiO_2)_n^-$ clusters with $n = 2-9$ corresponding to the neutral structures as shown in Figure 2. Other details are the same as in Figures 1 and 2.

in the same frequency range as in the spectra of rutile and anatase bulk. The excited electron and hole within each triplet structure tend to be localized on one of the least-coordinated Ti- and O-atoms, respectively, but are still subject to the electron−hole interaction. On the other hand, the extra electron in each $(TiO_2)_n^-$ clusters is localized mainly on the least

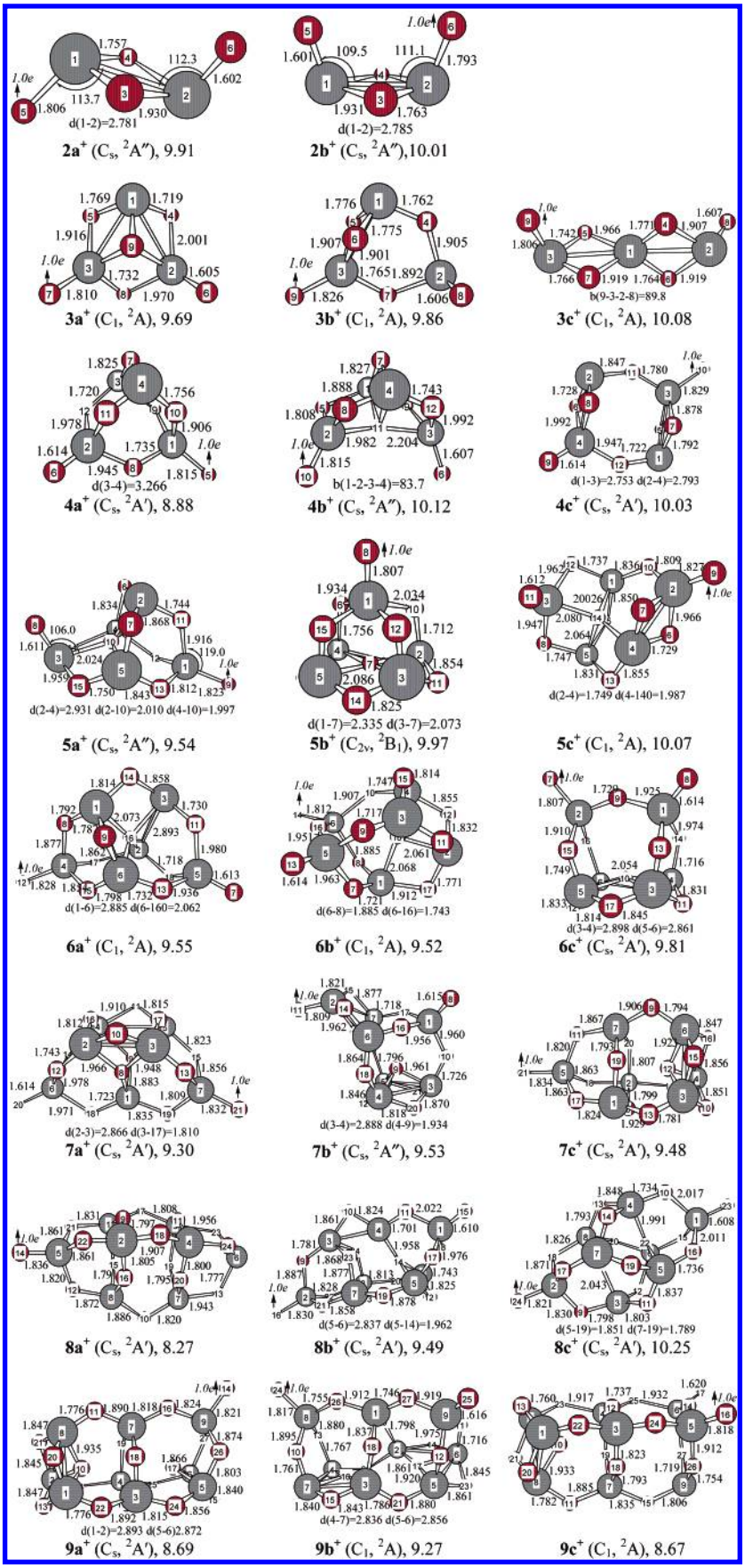

Figure 6. Geometries of negatively charged $(TiO_2)_n^+$ clusters with $n = 2-9$ corresponding to the neutral structures as shown in Figure 2. Other details are the same as in Figures 1 and 2.

coordinated Ti-atom(s), whereas the hole in each $(TiO_2)_n^+$ clusters is always on a terminal O-atom. The location of the hole on the terminal O-atom makes the $(TiO_2)_n^+$ clusters with $n = 1-9$ (Figure 6) unfit for studying photooxidation of water

on TiO_2. The predicted cluster formation energies, singlet−triplet gaps, ionization potentials and electron affinities agree well with the available experimental data. The results may be helpful for understanding the chemistry of small titanium dioxide clusters.

Acknowledgment. This work was supported by the NWO/ACTS hydrogen program. Z.-w.Q. thanks Prof. M. C. van Hemert for help with the Gaussian 03 program and Dr. R. A. Olsen for some helpful discussions.

References and Notes

(1) Grätzel, M. *Nature* **2001**, **414**, 338.
(2) Fujishima, A.; Honda, K. *Nature* **1972**, *238*, 37.
(3) Sato, S. *Chem. Phys. Lett.* **1986**, *123*, 126.
(4) Asahi, R.; Morikawa, T.; Ohwaki, T.; Aoki, K.; Taga, Y. *Science* **2001**, *293*, 269.
(5) Umebayashi, T.; Yamaki, T.; Itoh, H.; Asai, K. *Appl. Phys. Lett.* **2002**, *81*, 454.
(6) Ohno, T.; Mitsui, T.; matsumura, M. *Chem. Lett.* **2003**, *32*, 364.
(7) Khan, S. U. M.; Al-Shahry, M.; Ingler, W. B., Jr. *Science* **2002**, 297, 2243.
(8) Sakthivel, S.; Kisch, H. *Angew. Chem., Int. Ed.* **2003**, *42*, 4908.
(9) Hoffmann, M. R.; Martin, S. T.; Choi, W.; Bahnemann, D. *Chem. Rev.* **1995**, *95*, 69.
(10) Volodin, A. M. *Catal. Today* **2000**, 58, 103.
(11) Muscat, J.; Swamy, V.; Harrison, N. M. *Phys. Rev. B* **2002**, 65, 224112.
(12) Zhang, H.; Banfield, J. F. *J. Mater. Chem.* **1998**, *8*, 2073.
(13) Gail, H.-P.; Sedlmayr, E. *Faraday Discuss.* **1998**, *109*, 303.
(14) Nakamura, R.; Nakato, Y. *J. Am. Chem. Soc.* **2004**, *126*, 1290.
(15) Nakamura, R.; Tanaka, T.; Nakato, Y. *J. Phys. Chem. B* **2004**, *108*, 10617.
(16) Harris, L. A.; Quong, A. A. *Phys. Rev. Lett.* **2004**, *93*, 086105−1.
(17) Linsebigler, A.; Lu, G.; Yates, J. T., Jr. *Chem. Rev.* **1995**, *95*, 735.
(18) Matsuda, Y.; Bernstein, E. R. *J. Phys. Chem. A* **2005**, *109*, 314.
(19) Demyk, K.; van Heijnsbergen, D.; von Helden, G.; Meijer, G. *Astron. Astrophys.* **2004**, *420*, 547
(20) Yu, W.; Freas, R. B. *J. Am. Chem. Soc.* **1990**, *112*, 7126.
(21) Guo, B. C.; Kerns, K. P.; Castleman, A. W. *Int. J. Mass Spetrom., Ion Processes* **1992**, *117*, 129.
(22) Wu, H.; Wang, L.-S. *J. Chem. Phys.* **1997**, *107*, 8221.
(23) Albert, T.; Finocchi, F.; Noguera, C. *J. Chem. Phys.* **2000**, *113*, 2238.
(24) Albert, T.; Finocchi, F.; Noguera, C. *Faraday Discuss.* **1999**, *114*, 285.
(25) Albert, T.; Finocchi, F.; Noguera, C. *Appl. Surf. Sci.* **1999**, *144−145*, 672.
(26) Hagfeldt, A.; Bergström, R.; Siegbahn, H. O. G.; Lunell, S. *J. Phys. Chem.* **1993**, *97*, 12725.
(27) Bergström, R.; Lunell, S.; Eriksson, L. A. *Int. J. Quantum Chem.* **1996**, *59*, 427.
(28) Walsh, M. B.; King, R. A.; Schaefer, H. F., III. *J. Chem. Phys.* **1999**, *110*, 5224.
(29) Jeong, K. S.; Ch. Chang, Sedimayr, E.; Sülzle, D. *J. Phys. B: At. Mol. Opt. Phys.* **2000**, *33*, 3417.
(30) Persson, P.; Gebhardt, J. C. M.; Luneel, S. *J. Phys. Chem. B* **2003**, *107*, 3336.
(31) Hamad, S.; Catlow, C. R. A.; Woodley, S. M.; Lago, S.; Mejias, J. A. *J. Phys. Chem. B* **2005**, 109, 15741.
(32) Frisch, M. J.; Trucks, G. W.; Schlegel, H. B.; Scuseria, G. E.; Robb, M. A.; Cheeseman, J. R.; Montgomery, J. A., Jr.; Vreven, T.; Kudin, K. N.; Burant, J. C.; Millam, J. M.; Iyengar, S. S.; Tomasi, J.; Barone, V.; Mennucci, B.; Cossi, M.; Scalmani, G.; Rega, N.; Petersson, G. A.; Nakatsuji, H.; Hada, M.; Ehara, M.; Toyota, K.; Fukuda, R.; Hasegawa, J.; Ishida, M.; Nakajima, T.; Honda, Y.; Kitao, O.; Nakai, H.; Klene, M.; Li, X.; Knox, J. E.; Hratchian, H. P.; Cross, J. B.; Adamo, C.; Jaramillo, J.; Gomperts, R.; Stratmann, R. E.; Yazyev, O.; Austin, A. J.; Cammi, R.; Pomelli, C.; Ochterski, J. W.; Ayala, P. Y.; Morokuma, K.; Voth, G. A.; Salvador, P.; Dannenberg, J. J.; Zakrzewski, V. G.; Dapprich, S.; Daniels, A. D.; Strain, M. C.; Farkas, O.; Malick, D. K.; Rabuck, A. D.; Raghavachari, K.; Foresman, J. B.; Ortiz, J. V.; Cui, Q.; Baboul, A. G.; Clifford, S.; Cioslowski, J.; Stefanov, B. B.; Liu, G.; Liashenko, A.; Piskorz, P.; Komaromi, I.; Martin, R. L.; Fox, D. J.; Keith, T.; Al-Laham, M. A.; Peng, C. Y.; Nanayakkara, A.; Challacombe, M.; Gill, P. M. W.; Johnson, B.; Chen, W.; Wong, M. W.; Gonzalez, C.; Pople, J. A. *Gaussian 03*, revision C.02; Gaussian, Inc.: Wallingford, CT, 2004.
(33) Kohn, W.; Sham, L. J. *Phys. Rev.* **1965**, *140*, A1133.
(34) Becke, A. D. *J. Chem. Phys.* **1993**, *98*, 5648.
(35) Lee, C.; Yang, W.; Parr, R. G. *Phys. Rev. B* **1988**, *37*, 785.
(36) Dunning, T. H., Jr.; Hay, P. J. In *Modern Theoretical Chemistry*; Schaefer, H. F., III, Ed.; Plenum: New York, 1976; Vol. 3, p 1.
(37) Hay, P. J.; Wadt, W. R. *J. Chem. Phys.* **1985**, *82*, 270.
(38) Wadt, W. R.; Hay, P. J. *J. Chem. Phys.* **1985**, *82*, 284.
(39) Hay, P. J.; Wadt, W. R. *J. Chem. Phys.* **1985**, *82*, 299.
(40) Huber, K. P.; Herzberg, G. In *Molecular Spectra and Molecular Structure IV. Constants*; Van Nostrand Reihold: New York, 1979.
(41) Sappey, A. D.; Eiden, G.; Harrington, J. E.; Weisshaar, J. C. *J. Chem. Phys.* **1989**, *90*, 1415.
(42) McIntyre, N. S.; Thompson, K. R.; Weltner, W., Jr. *J. Phys. Chem.* **1971**, *75*, 3243.
(43) DeVore, T. C.; Gallaher, T. N. *High Temp. Sci.* **1983**, *16*, 269.
(44) Hildenbrand, D. L. *Chem. Phys. Lett.* **1976**, *44*, 281.
(45) Balducci, G.; Gigli, G.; Guido, M. *J. Chem. Phys.* **1985**, *83*, 1909.
(46) Balducci, G.; Gigli, G.; Guido, M. *J. Chem. Phys.* **1985**, *83*, 1913.
(47) *CRC handbook of Chemistry and Physics*, 82nd ed.; Lide, D. R.; CRC Press: Boca Raton, FL, 2002.
(48) The NIST Webbook of chemistry. See http://webbook.nist.gov/chemistry.
(49) Pascual, J.; Camassel, J.; Mathieu, H. *Phys. Rev. Lett.* **1977**, *39*, 1490.